

ISO–SWS Observations of CO₂ and H₂O in R Cassiopeiae^{*}

A.J. Markwick and T.J. Millar

Department of Physics, UMIST, P.O. Box 88, Manchester M60 1QD, UK

Received 21 March 2000 / Accepted 22 May 2000

Abstract. We present ISO–SWS spectra of the O-rich Mira variable R Cas, showing CO₂ in absorption and emission, and H₂O in absorption. The CO₂ absorption feature is the 01¹0 – 00⁰0 ro-vibrational band at 14.97 μm. The emission features are the 10⁰0–01¹0 and 11¹0 – 02²0 ro-vibrational transitions at 13.87 and 13.48 μm respectively. The water absorption spectrum shows the ν₁ and ν₃ ro-vibrational bands in the 2.75 – 3 μm region. Using LTE models, we derive physical parameters for the features. We find the CO₂ emission temperature to be ~ 1100 K. We discuss the nature of the CO₂ feature at 15 μm and show that it can be modeled as an emission/absorption band by deviating from thermal equilibrium for the population of the 01¹0 vibrational level. The H₂O absorption spectrum is shown to arise from gas at different temperatures, but can be fit reasonably well with two components at $T = 950$ K and $T = 250$ K. The CO₂ emission and hot H₂O absorption temperatures are similar, suggesting that these features probe the same region of the inner envelope. We discuss the inner envelope chemistry using molecular equilibrium calculations and recent modeling work by Duari et al. (1999), and find our observations consistent with the results.

We also report the detection of the CO₂ 01¹0 – 00⁰0 ro-vibrational band in absorption towards another oxygen-rich Mira, IRC+10011.

Key words: line: identification – stars: circumstellar matter – stars: individual: R Cas, IRC+10011 – infrared: stars

1. Introduction

R Cas is an O-rich Mira variable on the asymptotic giant branch (AGB). AGB stars undergo mass loss, with slow yet massive winds which return processed stellar material back into the interstellar medium. In this way they play a crucial role in as-

Send offprint requests to: A.J. Markwick
(ajm@janus1.phy.umist.ac.uk)

^{*} Based on observations with ISO, an ESA project with instruments funded by ESA Member States (especially the PI countries: France, Germany, the Netherlands and the United Kingdom) with the participation of ISAS and NASA. The SWS is a joint project of SRON and MPE.

trochemistry. Understanding the mass loss process is therefore important, and recent observations with ISO have made a significant contribution to our understanding.

In this paper, we report ISO–SWS observations of CO₂ in absorption and emission in R Cas. There have been several reported detections of carbon dioxide in AGB circumstellar envelopes with ISO, for example by Cami et al. (1997), Justtanont et al. (1998) and Ryde et al. (1999). Some of the CO₂ features which we have detected in R Cas have already been reported and discussed by these authors. However, our SWS spectra of R Cas have a much higher S/N than those previously presented. Also, we have a remarkably clean spectrum of IRC+10011 showing the first detection of the fundamental ν₂ ro-vibrational band in absorption towards this object. The previously reported observations of CO₂ in oxygen-rich AGB envelopes are summarised in Table 1.

We also report the detection of H₂O in absorption towards R Cas through its ν₁ and ν₃ ro-vibrational bands. The detection of water is one of the most remarkable ISO results, made possible by the telescope’s privileged position above the atmosphere. Previous ISO detections of water in AGB envelopes are of emission in R Cas (LWS; Truong-Bach et al. 1999) and absorption in NML Cyg (SWS; Justtanont et al. 1996). Table 2 summarises the physical parameters of R Cas.

2. Observations

The observations were made using the Short Wavelength Spectrometer (de Graauw et al. 1996) on board the Infrared Space Observatory (Kessler et al. 1996). The AOT06 observing template was used, which has a resolution of 1500. The observations formed part of a proposal to detect carbon-bearing molecules in oxygen-rich circumstellar envelopes (Markwick & Millar 1997). The regions of the spectrum observed were specifically chosen to include ro-vibrational bands of molecules such as methane, HCN, C₂H₂ and C₂H₆ in an attempt to learn more about the production and chemistry of carbon-bearing molecules in oxygen-rich circumstellar environments. We did not detect these species which will be the subject of a future paper as it remains to be seen if the data reduction for certain observing bands can be improved.

Table 1. Reported observations of CO₂ in O-rich Mira envelopes. References: Justtanont et al. 1998; Cami et al. 1997; Ryde et al. 1999. ‘E’ denotes feature seen in emission, ‘A’ absorption. *The fact that the CO₂ ν_2 fundamental at 14.97 μm seems to appear in both emission and absorption will be discussed further in Sect. 4. The detections reported in this paper are shown in bold type.

Band	μm	Object(s)	
11 ¹ 0 – 02 ² 0	13.48	EP Aqr, RX Boo, R Cen, R Cas	E E
10 ⁰ 0 – 01 ¹ 0	13.87	R Cas , W Hya, RX Boo, R Hya, R Cen, R Crt, R Dor	E E E
01 ¹ 0 – 00 ⁰ 0	14.97	RX Boo, EP Aqr, R Cas * R Cas *, W Hya, TX Cam, V1111 Oph, V656 Cas, IRC+10011	E A A A
01 ¹ 0 – 00 ⁰ 0	15.40	EP Aqr (¹³ CO ₂)	E
02 ⁰ 0 – 01 ¹ 0	16.18	R Cas, W Hya, RX Boo, R Hya, R Cen	E E

Table 2. Physical properties of R Cas. The values are taken from Haniff et al. (1995); Bujarrabal et al. (1994); Loup et al. 1993; Perryman et al. 1997.

Effective temperature	T_{eff}	2215 K
Stellar radius	R_*	2.0×10^{13} cm
Distance	D	106.7 ± 12 pc
Expansion velocity	v_e	14.3 km s^{-1}
Period	p	430 days
Mass loss rate	\dot{M}	$1.0 \times 10^{-6} \text{ M}_{\odot} \text{ yr}^{-1}$
Spectral type		M7IIIe
Chemical class		O

The observing band containing the 15 μm observations suffers severely from instrumental fringing, so this data was reduced using the SWS Interactive Analysis (IA) software package at SRON in Groningen. In the defringing process, an algorithm is used which mathematically removes the fringes by Fourier analysis. Because of its indiscriminating nature, care must be taken to ensure that real features are not removed by this method.

3. Spectral modeling

In order to derive the physical conditions in the absorbing and emitting gas we have made models using software to be included in the SWS IA package (Markwick & Lahuis, in preparation). The spectra were calculated using the following methods.

3.1. Absorption spectra

The synthetic absorption spectra were produced following Helmich (1996). For CO₂ and H₂O, the line positions were extracted from the HITRAN database (Rothman et al. 1992), which lists many lines in the bands we are considering here. The oscillator strengths f_j and the partition functions $Q(T)$ are

calculated from data tabulated in HITRAN, but since this calculation depends on the statistical weights of transitions, it is in general a slightly different process for each molecule. The remaining parameters for the model spectrum are then the column density N , the excitation temperature T , the envelope expansion velocity v_e and the instrumental resolution $R = \lambda/\Delta\lambda$. The expansion velocity is obtained from CO observations (eg. Loup et al. 1993). Assuming that the populations in each level can be characterized by a single excitation temperature, the column density in each line N_j can be calculated. Then the optical depth in each line is given by

$$\tau \sim N_j f_j \phi(\lambda - \lambda_0),$$

where $\phi(\lambda - \lambda_0)$ is a Voigt profile. In the calculation of the Voigt profile, we took the value referred to as the *doppler parameter* by some authors to be equal to the expansion velocity of the envelope.

The optical depths are converted to relative intensities via

$$y = e^{-\tau}.$$

The final spectrum is produced by mathematical convolution with a Gaussian profile whose width is equal to the instrumental resolution.

3.2. Emission spectra

The synthetic emission spectra were produced using a simple thermal model. The intensity of a line is given by

$$I_{ul} = N_u A_{ul} h\nu \text{ erg s}^{-1}$$

where N_u is the number of molecules in the upper level, A_{ul} is the Einstein coefficient and ν is the frequency of the line. If the molecules are in thermal equilibrium,

$$N_u = N_{\text{emit}} \left\{ \frac{g_u}{Q(T)} \right\} \exp\left(-\frac{E_u}{kT}\right)$$

where N_{emit} is the total number of emitting molecules, g_u is the statistical weight of the upper level, $Q(T)$ the partition function, T the temperature and E_u the energy of the upper level. The A_{ul} are calculated from the transition probabilities, a quantity which is tabulated in HITRAN.

The resulting spectrum is then converted to Janskys using the distance to the star D and the stellar radius R_* . The extent of the emitting region is calculated from the effective temperature of the star assuming a radial power law with index -0.6 for the temperature.

The model spectrum is completed, as in the case for absorption, by a convolution with a Gaussian instrumental profile.

4. Results and discussion

4.1. CO₂

In Fig. 1, we plot the 13–15 μm spectra we obtained for R Cas and IRC+10011. On comparison, we see that R Cas shows emission features not present in IRC+10011, and that the 15 μm feature has a different shape in R Cas.

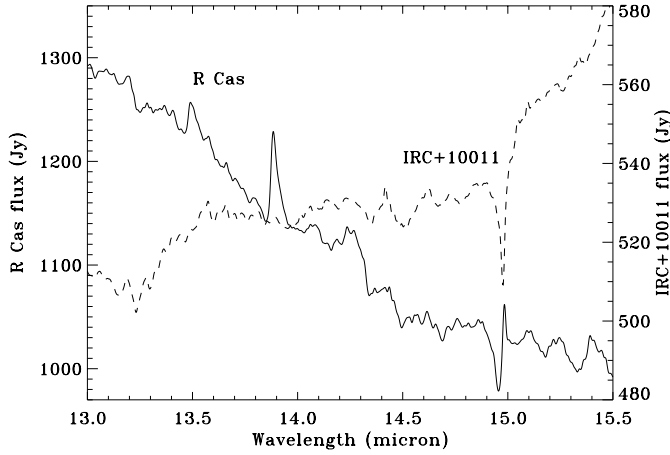


Fig. 1. The 13–15 μm spectra we obtained with ISO-SWS for R Cas and IRC+10011. CO₂ is in emission in the envelope of R Cas and not in that of IRC+10011, possibly due to the difference in mass loss rate between the two envelopes. The CO₂ feature at around 15 μm is different in R Cas due to the presence of bands in emission. In IRC+10011, this feature is solely due to the 01¹0–00⁰ (ν_2) absorption band.

That we see CO₂ emission features in R Cas and not in IRC+10011 could be due to the difference in mass loss rates for the two envelopes. Ryde et al. (1999) states that in envelopes with low mass loss, the possibility exists for gas to become trapped in a layer close to the star where it can get hot enough for the observed emission to occur. Where the mass loss rate is higher, no such possibility exists and so there are no emission features. Our observations are certainly consistent with this, as the mass loss rate of R Cas is about 100 times less than that of IRC+10011.

Fig. 2 shows the spectrum we obtained for R Cas of CO₂ in emission. The features are the Q-branches of the ro-vibrational bands 11¹0–02²0 and 10⁰0–01¹0 at 13.48 μm and 13.87 μm respectively (see Fig. 3). Table 3 gives the parameters used for all the model spectra presented in this paper. The model in Fig. 2 was made using a temperature $T = 1100$ K and number of emitting molecules $N_{\text{emit}} = 7 \times 10^{44}$. The resolution is 1000, reflecting the fact that the data was rebinned as part of the reduction process. The model temperature T has been calculated by considering the relative strengths of the Q-branches. We find $T = 1100 \pm 50$ K for the emitting gas, putting it at a radius of 6.4×10^{13} cm or about $3.2R_*$ from the star. The number of emitting molecules used to model the features can be converted into an average number density using

$$\langle n \rangle = \frac{N_{\text{emit}}}{\frac{4}{3}\pi(r^3 - R_*^3)}.$$

We find $\langle n_{\text{CO}_2} \rangle \approx 650 \text{ cm}^{-3}$.

At around 15 μm the main CO₂ feature is the ν_2 bending mode (see Fig. 3). The selection rules for this band are $\Delta J = 0, \pm 1$, giving rise to P, Q and R branches. Only the Q-branch is visible at the resolution of the ISO-SWS, due to the higher concentration of lines in it.

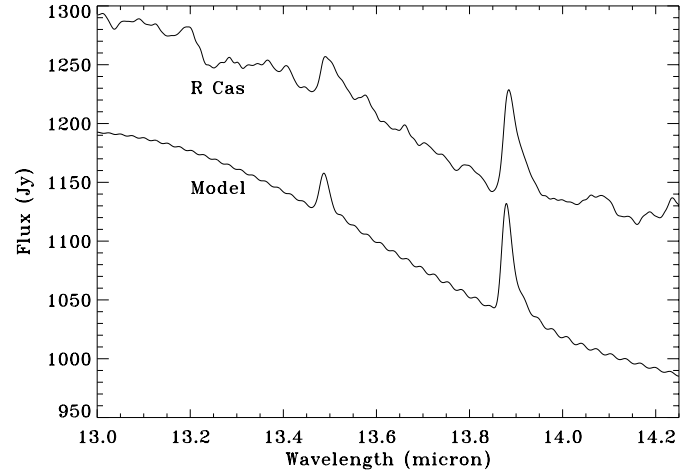


Fig. 2. Spectrum of R Cas, showing the Q-branches of CO₂ emission bands at 13.48 μm and 13.87 μm , together with a model spectrum, shifted for clarity. The model parameters are $T = 1100$ K, $N_{\text{emit}} = 7 \times 10^{44}$, $R = 1000$. The continuum is a 2215 K black body.

Table 3. Parameters used for the model spectra presented in this work. N is column density in cm^{-2} for absorption spectra (Type ‘A’) and the number of emitting molecules N_{emit} for emission (Type ‘E’) spectra. The figure captions give full information.

Fig.	Mol.	Type	T (K)	N	R
2	CO ₂	E	1100	7×10^{44}	1000
4	CO ₂	A	650	2.5×10^{16}	1000
5	CO ₂	E	1100	7×10^{44}	1000
6	CO ₂	E	1100	$10^{42} (N_u)$	1000
6	CO ₂	A	900	5×10^{16}	1000
8	CO ₂	A	650	2.75×10^{16}	1000
10	H ₂ O	A	950	8×10^{18}	1500
10	H ₂ O	A	250	6×10^{18}	1500

Justtanont et al. (1998) noted that this feature is seen shifted to the blue in R Cas by about 0.02 μm . Fig. 4 shows a model of this band, using a temperature $T = 650$ K and column density $N = 2.75 \times 10^{16} \text{ cm}^{-2}$. The temperature of the absorption was fixed by considering the width of the band - at higher T , more rotational levels are filled and so the profile spreads out to lower wavelengths. The peak absorption in the model spectrum is clearly not in the same place as in the spectrum of R Cas - it is shifted 0.02 μm to the blue. Therefore the model spectrum in Fig. 4 is not a model of the feature at all. Justtanont et al. suggest that the band can be satisfactorily modeled by including hot bands. We included the 02⁰0–01¹0 and 02²0–01¹0 bands in our model but cannot reproduce the observed spectrum by this approach alone.

It seems more likely that we are seeing absorption of the emission coming from closer to the star by the gas further out in the envelope. We have attempted to model this emission/absorption feature. Assuming vibrational LTE, and using the same parameters for the emission as required to fit the 13 μm bands, we get Fig. 5. The observed 15 μm feature cannot be reproduced like this for two reasons; the 01¹0–00⁰ emission

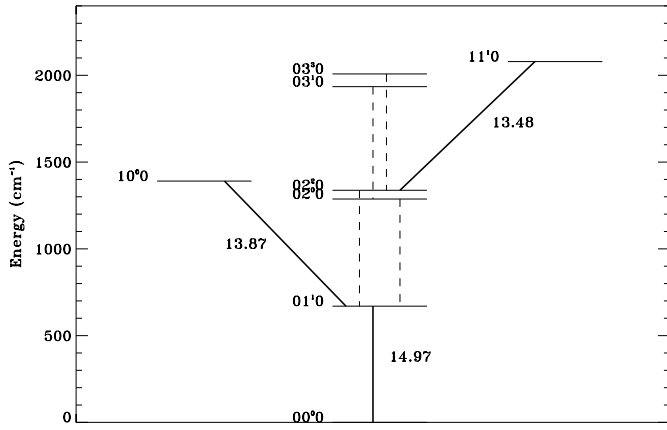


Fig. 3. Vibrational energy level structure of CO₂. The bands connected by solid lines are the ones we have detected in R Cas. The wavelength of each transition is shown in microns.

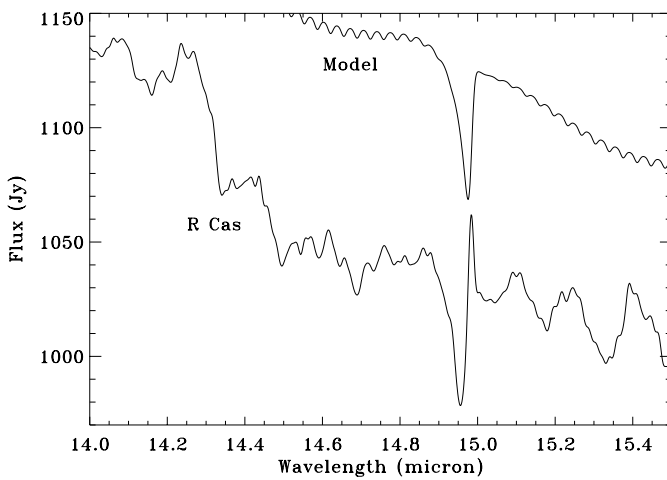


Fig. 4. Spectrum obtained of R Cas in the 15 μm region, together with a model spectrum of the Q-branch of the CO₂ fundamental ν_2 ro-vibrational band in absorption. The model parameters are $T = 650$ K, $N = 2.5 \times 10^{16}$ cm⁻², $R = 1000$. The continuum was fitted by eye, and the model spectrum is shifted in flux for clarity. It is clear that the feature is not fitted by this model. (see text).

is so strong that the column density required to absorb it is unreasonably large, and in addition, the shape of the feature is not fitted. If, however, we can deviate from a thermal population of the 01¹0 vibrational level, the strength of the emission at 15 μm can be reduced and we get the fit shown in Fig. 6. The parameters for the emission feature are $T = 1100$ K and $N_{01^10} \sim 10^{42}$, compared to $N_{01^10} \sim 10^{43}$ for the thermally populated case. For the absorption feature, $T = 900$ K and $N = 5 \times 10^{16}$ cm⁻². The full fit using this approach is shown in Fig. 7 - the agreement is excellent. The deviation from equilibrium could be caused by collisional de-excitation with H₂, by the preferential formation of CO₂ in excited states, or by a pumping mechanism. Alternatively, Ryde et al. (1999) suggest that the difference in relative strengths of the emission may be due to optical effects.

Fig. 8 shows the spectrum we obtained of IRC+10011 in the 15 μm region. Now the feature is not complicated by emission

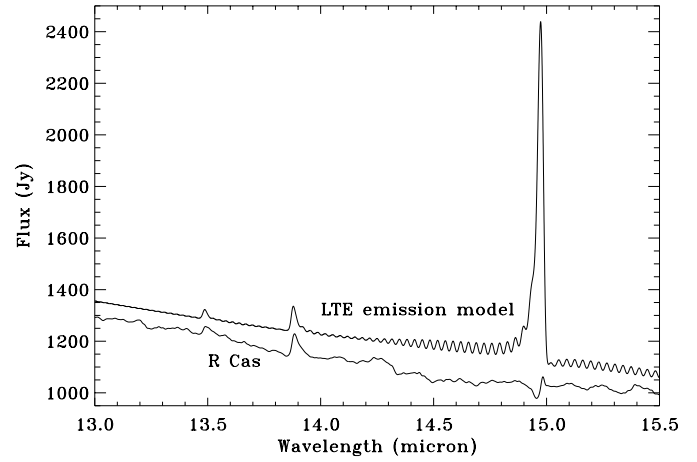


Fig. 5. A model of all of the R Cas CO₂ features, assuming LTE for the populations of the emitting vibrational levels. The emission due to the 01¹0 – 00⁰0 band is far too strong in this case to reproduce the observation. The model parameters are $T = 1100$ K, $N_{\text{emit}} = 7 \times 10^{44}$.

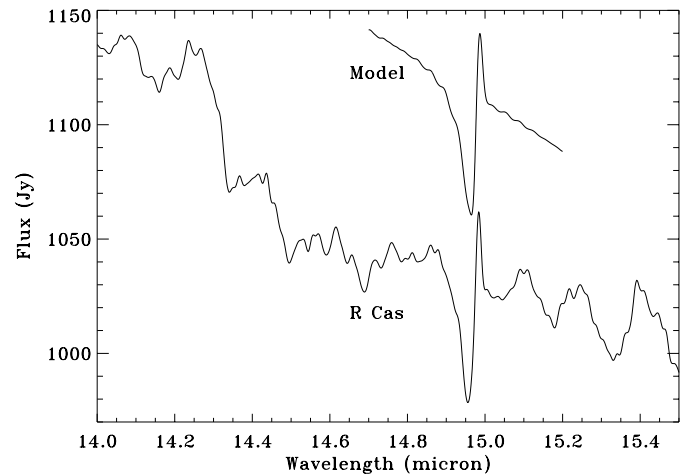


Fig. 6. The 15 μm feature in R Cas, with a model spectrum. The parameters are $T = 1100$ K, $N_u \sim 10^{42}$ for the emission bands, and $T = 900$ K, $N = 5 \times 10^{16}$ cm⁻² for the absorptions.

bands, so the fit is obtained using only the CO₂ 01¹0 – 00⁰0 band. We find the temperature of the band to be ≈ 650 K with column density $N = 3 \times 10^{16}$ cm⁻². Assuming a radial power law for the temperature in the envelope around IRC+10011, and taking $T_{\text{eff}} = 2100$ K, this puts the absorbing region of gas at about $7R_*$ from the star.

4.2. H₂O

Water is a triatomic non-linear planar symmetric molecule. It belongs to point group C_{2v} , so it can exist in two distinct forms, *ortho*-H₂O and *para*-H₂O. Levels in these different species have different statistical weights, and so care must be taken when working out the oscillator strengths. The ro-vibrational structure of the ν_3 mode for $J < 3$ is shown in Fig. 9.

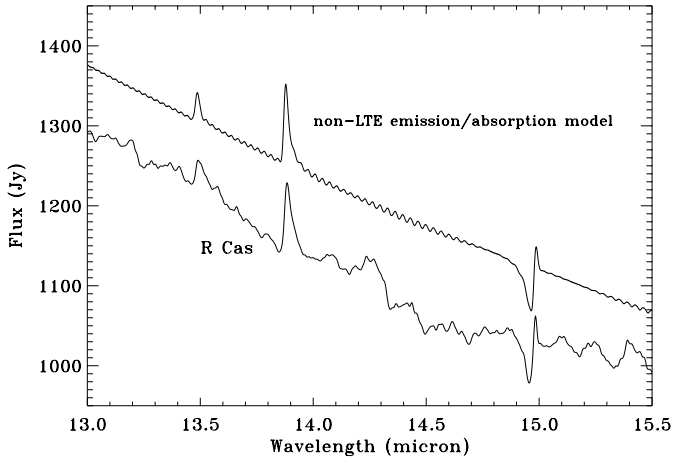


Fig. 7. A model of all of the R Cas CO₂ features, which deviates from thermal equilibrium for the 01¹0 – 00⁰0 emission band. The fit is excellent in this case. The parameters are as Fig. 2 for the 13 μm emission and as Fig. 6 for the other features.

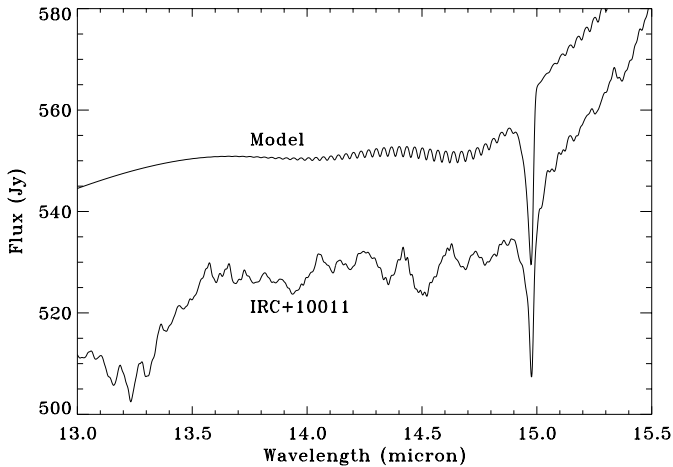


Fig. 8. Spectrum of IRC+10011, showing the CO₂ ν₂ Q-branch in absorption, together with a model spectrum, shifted in flux for clarity. The continuum was fitted by eye. The model parameters are $T = 650$ K, $N = 2.75 \times 10^{16}$ cm⁻², $R = 1000$.

The spectrum of R Cas showing water absorbing in its ν₁ symmetric stretch and ν₃ asymmetric stretch is shown in Fig. 10, together with a model spectrum. Due to the structure of the CO₂ bands we modeled above, raising the excitation temperature makes the feature spread out as higher J levels are populated. In the case of the H₂O bands, the main absorption features are *different* at different temperatures (see Fig. 11). For example, the features at 2.98–2.99 μm can only arise from hot gas, but the features around 2.75–2.80 μm can only arise from cold gas. In this way, one can decompose the observed spectrum into hot and cold components. We find that the main features of the spectrum can be reproduced using a two temperature model with a hot component at $T = 950 \pm 50$ K, corresponding to a radius of about $4R_*$, and a cold component at $T = 250 \pm 50$ K, corresponding to a radius of $40R_*$. This is the model shown in Fig. 10. The column densities in the two regions of gas are

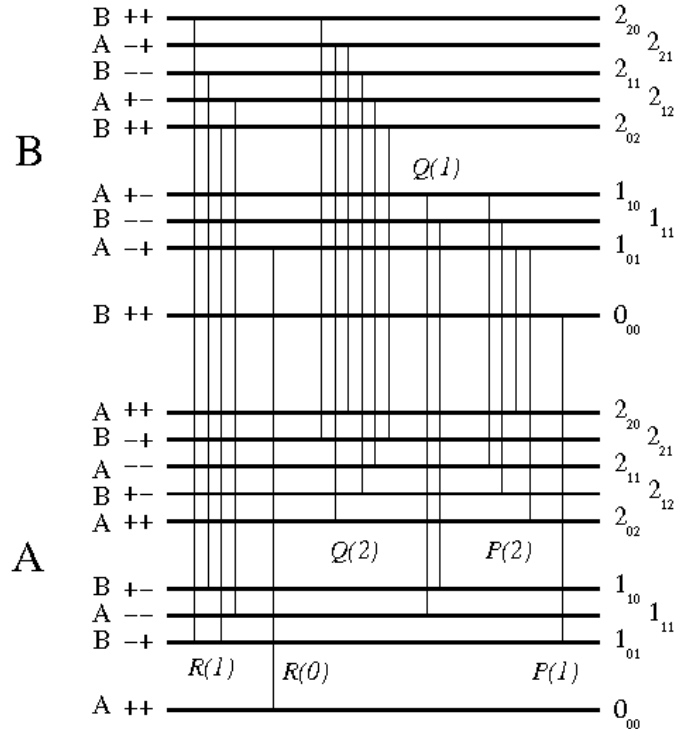


Fig. 9. The structure of the H₂O ν₃ ro-vibrational band for $J < 3$. The selection rules are $\Delta J = 0, \pm 1$, $J = 0 \not\leftrightarrow J = 0$, $++ \leftrightarrow --$, $+- \leftrightarrow -+$, $A \leftrightarrow A$, $B \leftrightarrow B$. Transitions connecting B levels (*ortho*-H₂O) are 3 times stronger than those connecting A levels (*para*-H₂O).

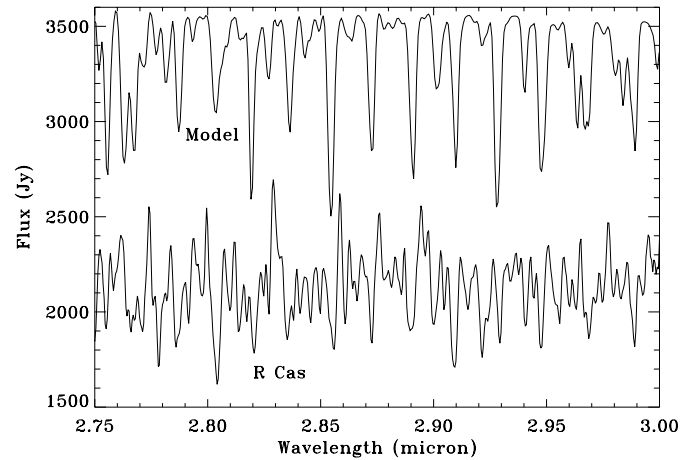


Fig. 10. Spectrum of R Cas (bottom) showing the ν₁ and ν₃ bands of water in absorption. The two temperature model parameters are $T = 950$ K, $N = 8 \times 10^{18}$ cm⁻², $T = 250$ K, $N = 6 \times 10^{18}$ cm⁻². The resolution $R = 1500$. The continuum is a 2215 K black body. The model has been shifted for clarity.

comparable ($\sim 10^{19}$ cm⁻²), which is consistent with the cold column being much longer than the hot one, as is demonstrably the case in a circumstellar envelope, assuming the temperature varies with radius according to a simple power law.

The temperature of the hot component of water absorption is similar to the temperature we find for the carbon dioxide emission features. This suggests that some of our CO₂ and

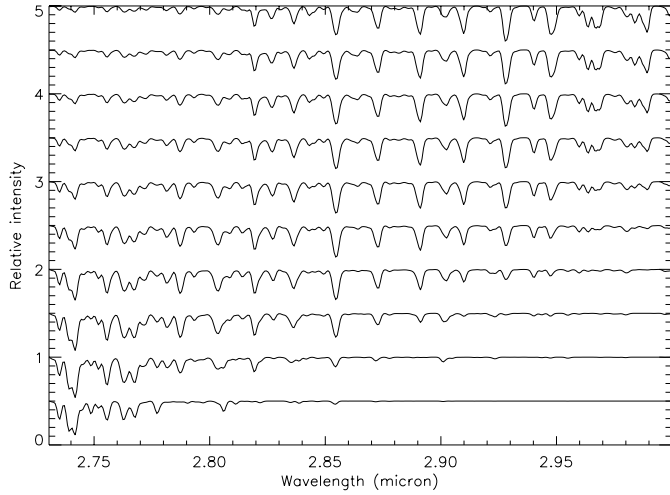


Fig. 11. Models of the H₂O ν_1 and ν_3 bands in absorption, from 100–1000 K (bottom to top). The spectra are shown shifted for clarity. The prominent features are different at different temperatures.

H₂O observations are probing the same region of the circumstellar envelope. The column density used in the model can be translated into an average number density by integrating $n(r)$ over the region of the envelope we are probing. We find $\langle n_{\text{H}_2\text{O}} \rangle \approx 7 \times 10^5 \text{ cm}^{-3}$. Now, using the previously obtained value for the number density of CO₂, we can estimate the $[\text{CO}_2] / [\text{H}_2\text{O}]$ ratio in the inner envelope, which we find to be $\approx 9 \times 10^{-4}$.

Also, we can crudely work out the mass loss rate of R Cas, using

$$\dot{M} = 4\pi r^2 n(r) v_e m_{\text{H}_2},$$

where r can be estimated from

$$\frac{r}{R_*} = \left(\frac{T_{\text{eff}}}{T} \right)^{5/3}.$$

The expansion velocity v_e derived from CO observations (see for example Loup et al. 1993) is the same as the expansion velocity of the whole envelope assuming that everything is coupled by collisions. The number density of hydrogen $n(r)$ is obtained from the column density of H₂O by assuming an abundance ratio $[\text{H}_2\text{O}] / [\text{H}_2]$ in the envelope of $f \sim 3 \times 10^{-4}$. In this way, we derive a mass loss rate of $\dot{M} \sim 10^{-6} M_{\odot} \text{ yr}^{-1}$, consistent with previous estimates.

4.3. Inner envelope chemistry

Our observations suggest that we are probing the inner region of the envelope, with $r < 5R_*$. To investigate what molecules are formed in the photospheres of stars, and therefore what kinds of species we should expect to find in the stars' inner envelopes, we have computed molecular equilibria. The calculation is performed by the method of steepest descent to minimise the Gibbs free energy of the gaseous mixture (White et al. 1958; Sharp & Huebner 1990). In the present calculation there are 211 molecular species. The results of this study for conditions appropriate

Table 4. The top 15 molecules produced in a molecular equilibrium calculation with parameters appropriate for R Cas. $f(X)$ is the fractional abundance of species X relative to total H nuclei. Also shown is the percentage of the total oxygen/carbon which is used up in making that species. $[a(b) = a \times 10^b]$

	X	$f(X)$	% O	% C
1	H ₂	8.25(-1)	-	-
2	CO	9.25(-4)	75.00	99.99
3	H ₂ O	2.42(-4)	19.65	-
4	N ₂	1.07(-4)	-	-
5	SiO	5.72(-5)	4.64	-
6	OH	7.39(-6)	5.99(-1)	-
7	SH	6.35(-6)	-	-
8	H ₂ S	5.92(-7)	-	-
9	HCl	2.84(-7)	-	-
10	SiS	1.61(-7)	-	-
11	HF	1.40(-7)	-	-
12	TiO	1.33(-7)	1.08(-2)	-
13	PO	8.00(-8)	6.48(-3)	-
14	NP	6.80(-8)	-	-
15	CO ₂	5.17(-8)	8.39(-3)	5.59(-3)

for R Cas are presented in Table 4. The physical conditions for the gas were; temperature $T = 2215 \text{ K}$; C/O ratio = 0.75; total pressure $P = 1.033 \times 10^{-3} \text{ atm}$, corresponding to a density of hydrogen nuclei of $3 \times 10^{15} \text{ cm}^{-3}$. We assumed solar metallicity for oxygen.

In Table 4, the molecules are listed in order of the absolute abundance produced. From this, we see that water is the third most abundant molecule produced, with an abundance of 2.42×10^{-4} relative to total H nuclei. Water also consumes 19.65% of all the oxygen. CO₂ has a lower abundance, but is the second greatest consumer of carbon after CO which takes the majority.

From these numbers, we arrive at $[\text{CO}_2] / [\text{H}_2\text{O}] \approx 2 \times 10^{-4}$ in the photosphere of R Cas, a little lower than the value we obtained for the inner envelope from our modeling of the observations. However, recent modeling work by Duari et al. (1999) has shown that shocks induced by stellar pulsations can enhance the abundances of some species in the inner envelopes of Mira variables. R Cas has a low mass loss rate, and so the possibility exists for material to become trapped in a layer close to the star, allowing such chemical enhancement to occur. CO₂ is a species whose abundance is particularly affected in their models. It is formed by OH, from the collisional destruction of water by atomic hydrogen, going on to react with CO. The net result of this is that CO₂ is formed at the expense of water, so the ratio of CO₂ to H₂O is increased, typically to a value of around 10^{-3} . This is in good agreement with our observed value. The model of Duari et al. is based on a molecular equilibrium calculation exactly like the one we described above, suggesting that while molecular equilibrium has been shown to be a poor approximation in the innermost regions of the envelope for some species like SO₂ (Yamamura et al. 1999), it can be good for other molecules. It is particularly interesting to note that nearly all of

the molecules in Table 4 have been observed in O-rich AGB circumstellar envelopes.

5. Conclusion

We have clearly detected CO₂ absorption, CO₂ emission and H₂O absorption in our spectra of R Cas. In IRC+10011, we have detected CO₂ absorption. To model the features we used LTE models, and found that the IRC+10011 carbon dioxide spectrum appears to arise from 650 K gas with column density $N = 3 \times 10^{16} \text{ cm}^{-2}$. The R Cas CO₂ emission can be fit with $T = 1100 \text{ K}$, $N = 2 \times 10^{16} \text{ cm}^{-2}$, indicating that we are probing the innermost regions of the envelope. We have demonstrated that the feature at $15 \mu\text{m}$ is an emission/absorption feature, and that it can only be fitted well if a deviation from thermal population of the 01¹⁰ vibrational level is made. This deviation could be caused by collisional de-excitation with H₂, by the preferential formation of CO₂ in excited states, or by a pumping mechanism, for example.

The H₂O spectrum appears to contain contributions from hot ($T \approx 950 \text{ K}$) and cold ($T \approx 250 \text{ K}$) gas.

Using our models to estimate the ratio $[\text{CO}_2] / [\text{H}_2\text{O}]$ in the inner envelope of R Cas gives a value of 9×10^{-4} . This is consistent with LTE formation of CO₂ and H₂O, but with CO₂ formation enhanced by shock chemistry induced by stellar pulsations, as modeled by Duari et al. (1999).

Acknowledgements. Research in Astrophysics at UMIST is supported by PPARC. AJM is grateful for the award of a studentship from PPARC. Many thanks to Fred Lahuis of SRON, Groningen for help reducing the data.

References

- Bujarrabal V., Fuente A., Omont A., 1994, A&A 285, 247
 Cami J., Justtanont K., de Jong T., et al., 1997, in: Heras A.M., et al. (eds.), Proceedings of the first ISO Workshop on Analytical Spectroscopy, ESA, p. 159
 de Graauw Th., Haser L.N., Beintema D.A., et al., 1996, A&A 315, L49
 Duari D., Cherchneff I., Willacy K., et al., 1999, A&A 341, L47
 Haniff C.A., Scholz M., Tuthill P.G., 1995, MNRAS 276, 640
 Helmich F.P., 1996, PhD thesis, Leiden
 Justtanont K., de Jong T., Helmich F.P., et al., 1996, A&A 315, L217
 Justtanont K., Feuchtgruber H., de Jong T., et al., 1998, A&A 330, L17
 Kessler M.F., Steinz J.A., Anderegg M.E., et al., 1996, A&A 315, L27
 Loup C., Forveille T., Omont A., Paul J.F., 1993, A&AS 99, 291
 Markwick A.J., Millar T.J., 1997, ApSS 251, 255
 Perryman M.A.C., Lindegren L., Kovalevsky J., et al., 1997, A&A 323, L49
 Rothman L.S., Gamache R.R., Goldman A., et al., 1992, App. Optics 26, 4058
 Ryde N., Eriksson K., Gustafsson B., 1999, A&A 341, 579
 Sharp C.M., Huebner W.F., 1990, ApJS 72, 417
 Truong-Bach, Sylvester R.J., Barlow M.J., et al., 1999, A&A 345, 925
 White W.B., Johnson W.M., Dantzig G.B., 1958, JChPh 28, 751
 Yamamura I., de Jong T., Onaka T., et al., 1999, A&A 341, L9